

NEW SPECTRAL AND ABUNDANCE FEATURES OF INTERPLANETARY HEAVY IONS IN COROTATING INTERACTION REGIONS

G. M. MASON,¹ J. E. MAZUR, AND J. R. DWYER

Department of Physics, University of Maryland, College Park, MD 20742; mason@sampx3.umd.edu, mazur@sampx3.umd.edu, dwyer@umstep.umd.edu

AND

D. V. REAMES AND T. T. VON ROSENVINGE

NASA/Goddard Space Flight Center, Greenbelt, MD 20771; reames@lheavx.gsfc.nasa.gov, tycho@rosserv.gsfc.nasa.gov

Received 1997 April 18; accepted 1997 June 18

ABSTRACT

We have surveyed the composition and energy spectra of heavy ions accelerated in 17 corotating interaction regions (CIRs) during solar minimum conditions between 1992 December and 1995 July. Using new high-sensitivity instruments on *WIND* and *SAMPEX*, we are able to cover the energy range from approximately 20 keV nucleon⁻¹ to greater than 10 MeV nucleon⁻¹, making it possible to distinguish differing forms of particle spectra. Previous measurements down to about 0.5 MeV nucleon⁻¹ found exponential energy spectra; however, at the even lower energies studied here, we find that the spectral forms become power laws in kinetic energy per nucleon. At 150 keV nucleon⁻¹ we find that the C:O and Ne:O ratios depend on solar wind speed. These variations suggest that in addition to the solar wind, other sources of heavy ions contribute to the CIR composition.

Subject headings: acceleration of particles — cosmic rays — interplanetary medium — solar wind

1. INTRODUCTION

Corotating interaction regions (CIRs) were first observed in the 1960s as periods of enhanced interplanetary flux levels of about 1 MeV nucleon⁻¹ ions that reappeared in successive solar rotations. When the *Pioneer 10/11* deep space probes moved well beyond Earth orbit in the mid-1970s, it was discovered that these enhanced fluxes did not originate at the Sun, but rather in interaction regions between fast and slow solar wind streams (e.g., Barnes & Simpson 1976; McDonald et al. 1976). A theoretical model by Fisk & Lee (1980) explained the events in terms of acceleration of solar wind ions at forward and reverse shocks bounding the interaction region, with propagation back to 1 AU including adiabatic deceleration.

High-sensitivity energetic particle instrumentation on the recently launched *WIND* and *SAMPEX* satellites makes it possible to study the particle spectra to much lower energies than prior work. In addition, the newly available detailed solar wind abundances measured on *Ulysses* (Gloeckler et al. 1992) allow much more detailed comparisons with solar wind abundances than was possible earlier. For the energetic particles, we find that (1) the CIR energy spectra continue to rise as power laws below about 100 keV nucleon⁻¹, rather than rolling off as an exponential in velocity as predicted by the theory of Fisk & Lee (1980); (2) the abundances are close to the solar wind values *averaged* between the high- and low-speed solar wind streams; and (3) there is a strong increase in the C/O and Ne/O ratios with increasing solar wind speed, even though this behavior is not observed for other ratios, such as He/O and Mg/O. These new observations require additional mechanisms to describe the acceleration and transport of CIR ions to 1 AU and may point to the existence of new, unknown ion sources in the region of 1–5 AU, where the CIR acceleration is strongest.

2. OBSERVATIONS

The new energetic particle observations presented here were obtained with the Low-energy Ion Composition Analyzer (LICA) instrument on the *SAMPEX* spacecraft (Mason et al. 1993), and the Energetic Particle Acceleration, Composition, and Transport (EPACT), Supra-Thermal through Energetic Particle, (STEP) and Low Energy Matrix Telescope (LEMT) telescopes on the *WIND* spacecraft (von Rosenvinge et al. 1995). Solar wind speed information from *Interplanetary Monitoring Platform (IMP) 8* was obtained from the National Space Science Data Center for periods prior to the launch of *WIND*, and from the *WIND* Solar Wind Experiment (SWE) instrument thereafter. During the current solar minimum, numerous CIRs have been observed, and the present survey emphasizes those with the largest energetic particle enhancements from the launch of *SAMPEX* in 1992 July, until the end of 1995. The 17 events in this survey are listed in Table 1. They were identified by their association with high-speed solar wind streams and lack of temporal dispersion in the onset for particles of different energy. For the *WIND* observations, some CIR events had periods when upstream ions were present (e.g., Mason, Mazur, & von Rosenvinge 1996): these upstream events were identified by their short timescales and were removed from the analysis presented here (the ~1 MeV nucleon⁻¹ *SAMPEX* observations from low Earth orbit are not subject to contamination from upstream events).

Figure 1 shows *WIND* observations of one of the larger events in the list (number 7, starting 1994 December 6). Note the increase in solar wind speed accompanied by increases in the He fluxes in energy bins centered approximately at 60, 240, 950, 1930, 2850, and 5600 keV nucleon⁻¹. Higher energy fluxes reach their peak values after the lower energies (e.g., at 950 keV nucleon⁻¹ the peak occurs about 12 hr after the peak at 60 keV nucleon⁻¹). Thus, the energy spectra harden significantly

¹ Also Institute for Physical Science and Technology.

TABLE 1
COROTATING INTERACTION REGION EVENTS IN SURVEY

Number	Onset Date	Number	Onset Date
1	1992 Dec 8	10	1995 Feb 12
2	1993 Jan 3	11	1995 Apr 7
3	1994 Jan 11	12	1995 Apr 26
4	1994 Feb 7	13	1995 May 2
5	1994 Oct 2	14	1995 May 24
6	1994 Nov 25	15	1995 May 30
7	1994 Dec 6	16	1995 Jun 19
8	1995 Jan 1	17	1995 Jul 16
9	1995 Jan 29		

Note.—Numbers 1–5 and 7 were observed with the *SAMPEX* satellite over the polar caps; numbers 6–17 were observed with *WIND*.

during the event. Time-intensity profiles for heavier ions such as C+N+O show similar behavior.

Figure 2 shows energy spectra for a 24 hr period beginning 18:00 on 1994 December 6 (day 340; see hatched box in Fig. 1). The spectra are typical of the events in the survey. Below about 1 MeV nucleon⁻¹, the species shown are H, He, C+N+O, and the Fe group. Above 2 MeV nucleon⁻¹, He, C, and O are shown. Note that the low-energy spectra continue to rise as power laws down to the instrument threshold of about 30 keV nucleon⁻¹. Above 1 MeV nucleon⁻¹ the spectra steepen significantly, as in the Fisk & Lee (1980) model; the “bump” in the spectra above about 10 MeV nucleon⁻¹ is due to anomalous component He and O.

In order to explore possible changes in high- to low-first ionization potential (FIP) element abundances in CIRs, we examined the Mg/O ratio at 70 keV nucleon⁻¹ for all the events observed by STEP. Figure 3 shows a sample result for

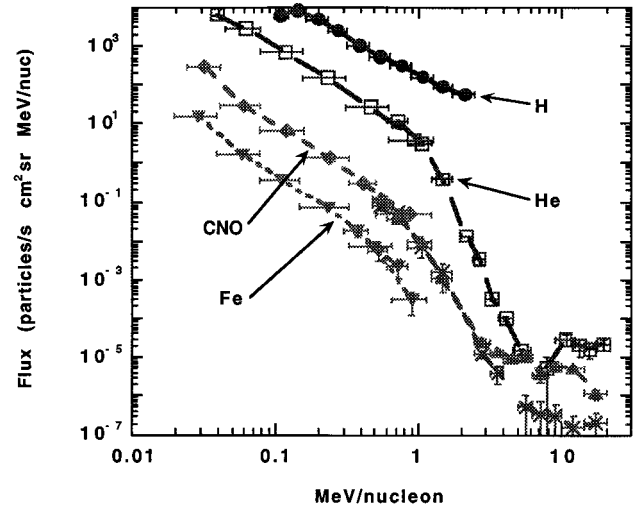


FIG. 2.—Energy spectra for the 24 hr period starting 1994 December 6, 18:00 UT. Note power-law spectra at low energies, rolling over above about 1 MeV nucleon⁻¹.

event 15, with the top panel showing the O flux. The stream interface (SI) passage at about day 150.18 (arrow) divides the ions from the forward and reverse shocks and is coincident with a sharp dip in the oxygen flux. The bottom panel compares the Mg/O ratio to the range of *Ulysses* solar wind Mg/O ratios, denoted by a shaded box in which the low-speed solar wind valve is at the top and the high-speed value at the bottom. Note that the Mg/O ratio at 70 keV nucleon⁻¹ shows

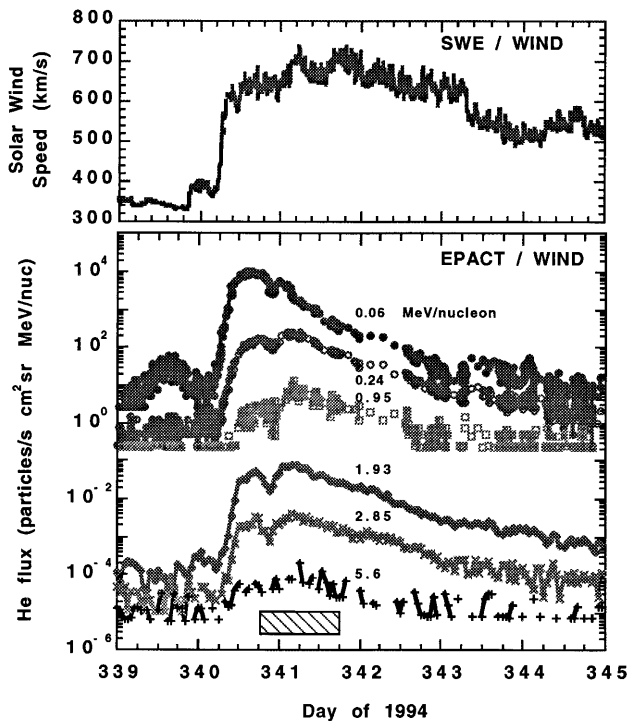


FIG. 1.—Solar wind speed (top) and selected He fluxes (bottom) for the CIR starting 1994 December 6. Note that low-energy fluxes rise before higher energies. Hatched box shows time averaging interval used for Fig. 2.

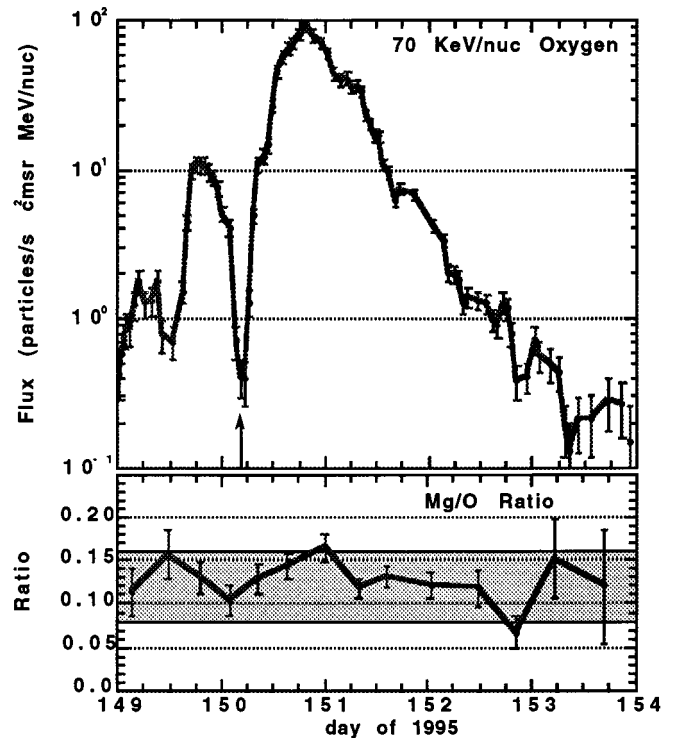


FIG. 3.—Top: Time-intensity profile of 70 keV nucleon⁻¹ O fluxes during CIR 15. The arrow marks stream interface. Bottom: The 6 hr average Mg/O ratio at 70 keV nucleon⁻¹. Shaded area shows range of *Ulysses* solar wind Mg/O for slow solar wind (upper edge of panel) and fast solar wind (lower edge of panel). Average solar wind speed during this event is 666 km s⁻¹.

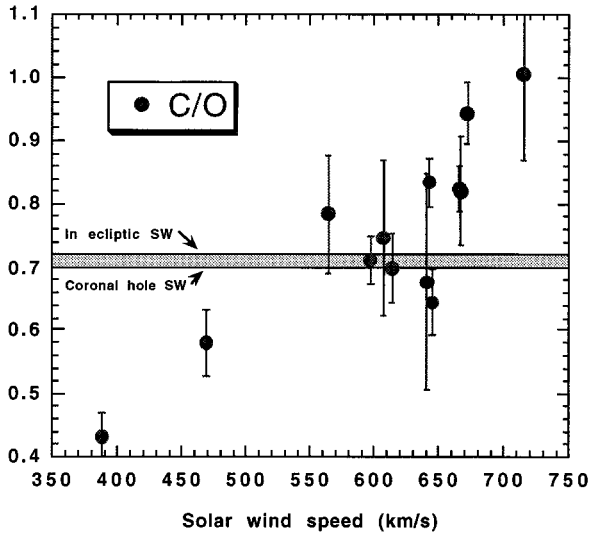


FIG. 4.—The 150 keV nucleon⁻¹ C/O abundance in 12 CIRs vs. solar wind speed during the event. Shaded area shows range of solar wind C/O ratios for slow vs. fast solar wind streams.

no particular time dependence during the event but remains near the average of (Mg/O)_{fast} and (Mg/O)_{slow}.

Figure 4 shows the C/O ratio at 150 keV nucleon⁻¹ for each of the 12 CIRs observed on *WIND* plotted versus the average solar wind speed during the event. The shaded area shows the range of solar wind ratios for fast- and slow-speed streams. Note the strong increase in C abundance compared with O as the solar wind speed increases, rising from well below to well above the average solar wind value of about 0.7 (von Steiger & Geiss 1995). This behavior is also seen for Ne/O, which increases with solar wind speed, and possibly also for Fe/O. In contrast, the He/O, Mg/O, and Si/O ratios at 150 keV nucleon⁻¹ show no systematic variation with solar wind speed.

Table 2 lists abundances normalized to O for mean energies of 150 keV nucleon⁻¹ (STEP) and about 1 MeV nucleon⁻¹ (LICA). The energetic particle composition for these events was averaged over the maximum flux intensities in each event, with time period lengths ranging from 12 to 48 hr, depending on the event's time-intensity profile. For comparison, *Ulysses* solar wind abundances are shown in the table for "in ecliptic"

and "coronal hole" values, corresponding roughly to low- and high-speed solar wind streams.

3. DISCUSSION

The spectral forms observed here roll over above 1–2 MeV nucleon⁻¹ as predicted by the Fisk & Lee (1980) model. However, the continued rise at low energies is not predicted by the numerical model of Fisk & Lee (1980), which yields spectra that are exponentials in velocity that also roll over toward low energies when plotted as kinetic energy power laws, while the present measurements find power-law increases continuing down to the instrument threshold near 30 keV nucleon⁻¹. This might be an effect related to the hardening of spectra seen in these events and suggests that at 1 AU the low-energy particles may be coming from portions of the CIR closer to Earth than for the higher energies.

One of the key new results from the *Ulysses* solar wind composition measurements has been the discovery that the enhancement of low-FIP elements is much smaller in solar wind high-speed streams than in the slower solar wind observed in the ecliptic (e.g., Geiss et al. 1995; von Steiger & Geiss 1995). Since CIRs span a transition between low-speed and high-speed solar wind streams, a change in the solar wind composition would be expected between high- and low-FIP elements such as O (FIP = 13.62 eV) and Mg (FIP = 7.65 eV). Indeed, in an analysis of seven CIRs observed on *Ulysses* near 5 AU, Wimmer Schweingruber, von Steiger, & Paerli (1997) have reported a decrease in the Mg/O ratio by a factor of about 2 between the pre-fast stream period in CIRs and the post-SI interface periods. This might result in a systematic change in the composition at higher energies and in any case should be considered when comparing energetic particle abundances in CIRs with solar wind abundances. However, as shown in Figure 3, the Mg/O ratio at 70 keV nucleon⁻¹ shows no variation during the CIR, and this is typical of the 12 CIRs observed by STEP during this survey.

Not only is the Mg/O ratio essentially constant during the CIRs, but its absolute value is characteristic of neither the high-speed solar wind stream value nor the low-speed stream value. Rather (see Fig. 3), the observed Mg/O is close to the simple average between the high- and low-speed stream values. Column (6) of Table 2 contains the average high- and low-speed solar wind values in the table, and columns (7) and

TABLE 2
COROTATING INTERACTION REGIONS AND SOLAR WIND ABUNDANCES

Element (1)	STEP ^a (150 keV nucleon ⁻¹) (2)	LICA ^b (1 MeV nucleon ⁻¹) (3)	Solar Wind Coronal Hole ^a (4)	Solar Wind in Ecliptic ^c (5)	Solar Wind Average (low + high) (6)	STEP/SW Average (low + high) (7)	LICA/SW Average (low + high) (8)
H	907 ± 444	...	1590 ± 500	1900 ± 400	1745 ± 320	0.52 ± 0.27	...
He	113 ± 20	211 ± 17	83 ± 25	75 ± 20	79 ± 16	1.43 ± 0.39	2.67 ± 0.58
C	0.75 ± 0.12	0.94 ± 0.07	0.70 ± 0.10	0.72 ± 0.10	0.71 ± 0.07	1.05 ± 0.20	1.33 ± 0.17
N	0.15 ± 0.04	0.15 ± 0.01	0.13 ± 0.01	0.14 ± 0.01	...	1.09 ± 0.27
O	=1	=1	=1	=1	=1	=1	=1
Ne	0.21 ± 0.05	0.17 ± 0.02	0.14 ± 0.01	0.14 ± 0.02	0.14 ± 0.01	1.53 ± 0.41	1.24 ± 0.17
Mg	0.13 ± 0.03	0.10 ± 0.02	0.08 ± 0.02	0.16 ± 0.03	0.12 ± 0.02	1.05 ± 0.27	0.81 ± 0.17
Si	0.11 ± 0.02	0.08 ± 0.01	0.05 ± 0.01	0.19 ± 0.04	0.12 ± 0.02	0.91 ± 0.25	0.66 ± 0.15
S	0.03 ± 0.01	0.02 ± 0.00	0.04 ± 0.01	0.03 ± 0.00	...	0.98 ± 0.32
Fe	0.08 ± 0.03	0.10 ± 0.01	0.06 ± 0.01	0.12 ± 0.03	0.09 ± 0.02	0.89 ± 0.42	1.07 ± 0.23

^a Events 1–5 in Table 1.
^b Events 6–17 in Table 1.
^c Table 1 of von Steiger & Geiss 1995.

(8) contain the ratio of the STEP and LICA averages to the column (6) values. The energetic particle abundances at 150 keV nucleon⁻¹ from *WIND* and the approximately 1 MeV nucleon⁻¹ values from LICA are generally consistent, within uncertainties, with this “average” solar wind abundance, with the notable exception of Ne. Note that if we had used either high-speed or low-speed solar wind values by themselves, then the low-FIP element abundances (Mg, Si, and Fe) would change by about 50%, and the agreement would not be satisfactory.

The increase of the C and Ne abundance with respect to O as a function of solar wind speed is difficult to understand if the energetic particles are accelerated out of the solar wind, since these elements have similar masses and charge-to-mass ratios. Richardson et al. (1993) observed changes in 1.9–2.8 MeV nucleon⁻¹ CIR abundance ratios, reporting increases in He/O and C/O with solar wind speed, and possible decreases in Fe/O and Mg/O ratios; in contrast to the result at 150 keV nucleon⁻¹ presented here, they did not observe a change in the Ne/O ratio with solar wind speed. They suggested that the observed ratio changes were due to changes in solar wind composition with solar wind speed. With the detailed measurements now available from *Ulysses*, it is clear that while the solar wind composition does show variations between the low- and high-speed streams, these variations are much less than the variations in the CIR energetic particle C:O and Ne:O ratios reported here.

Since the STEP observations fall within an 8 month period during solar minimum, a solar cycle origin of the C/O increase with solar wind speed is ruled out. In addition, the fact that the energetic particle abundances do not reflect the clear variation of solar wind Mg/O during the passage of the CIR (von Steiger & Geiss 1995) also shows that the changes in the solar wind abundance as the CIR passes a point at several AU are not seen in the energetic particles at Earth orbit. Of course, it is

possible that such variations could be masked by mixing of the particle populations as they propagated in to 1 AU. However, the SI in the CIR is an effective barrier to the energetic particles, as shown e.g., by the strong decrease in intensity in Figure 3 coincident with the SI passage (Intriligator & Siscoe 1994). This would argue against the mixing of slow and fast stream Mg/O ratios, and so it must be noted that the agreement between the *WIND* energetic ion abundances and the *average* of the slow and fast stream values is puzzling.

Recently, Gloeckler et al. (1994) and Geiss et al. (1994) have reported interstellar pickup H⁺, He⁺, O⁺, and N⁺ observed on *Ulysses* at distances of several AU. It is known that pickup ions show significant changes in relative abundances in the range of 1–5 AU, and we note that this variation occurs in the same region where the CIRs reach their peak intensities. However, the ionization states of heavy ions observed at 1 AU in CIRs show only small abundances of low-charge states and so do not appear to be dominated by sources such as pickup ions (Chotoo, Galvin, & Gloeckler 1996). If the C/O and Ne/O enhancements with solar wind speed are a signature of pickup ions of unknown source, then the abundances may increase with increasing solar wind speed, since the maximum pickup ion velocity scales directly with solar wind speed, thereby favoring injection in cases in which the solar wind speed is higher. While the ionization state information rules out any simple mechanism involving pickup ions, we speculate that the CIR abundances here may point to a new source of enhanced C and Ne in the range of 1 to a few AU.

We thank K. Ogilvie and the SWE team for the solar wind data used here. We benefited from discussions with I. G. Richardson and from the 1996 and 1997 CIRs workshops held at Elmau, Germany. This work was supported in part by NASA grants NAG 5-2865 and NAG 5-2963.

REFERENCES

- Barnes, C. W., & Simpson, J. A. 1976, *ApJ*, 210, L91
 Chotoo, K., Galvin, A. B., & Gloeckler, G. 1996, *Trans. Am. Geophys. Union*, 77, S212
 Fisk, L. A., & Lee, M. A. 1980, *ApJ*, 237, 620
 Geiss, J., Gloeckler, G., Mall, U., von Steiger, R., Galvin, A. B., & Ogilvie, K. W. 1994, *A&A*, 282, 924
 Geiss, J., et al. 1995, *Science*, 268, 1033
 Gloeckler, G., et al. 1992, *A&AS*, 92, 267
 ———. 1994, *J. Geophys. Res.*, 99, 17637
 Intriligator, D. S., & Siscoe, G. L. 1994, *Geophys. Res. Lett.*, 21, 1117
 Mason, G. M., Hamilton, D. C., Walpole, P. H., Heuerman, K. F., James, T. L., Lennard, M. H., & Mazur, J. E. 1993, *IEEE Trans. Geosci. & Remote Sensing*, 31, 549
 Mason, G. M., Mazur, J. E., & von Rosenvinge, T. T. 1996, *Geophys. Res. Lett.*, 23, 1231
 McDonald, F. B., Teegarden, B. J., Trainor, J. H., von Rosenvinge, T. T., & Webber, W. R. 1976, *ApJ*, 203, L149
 Richardson, I. G., Barbier, L. M., Reames, D. V., & von Rosenvinge, T. T. 1993, *J. Geophys. Res.*, 98, 13
 von Rosenvinge, T. T., et al. 1995, *Space. Sci. Rev.*, 71, 155
 von Steiger, R., & Geiss, J. 1995, in *Cosmic Winds and the Heliosphere*, ed. J. R. Jokipii, C. P. Sonnett, & M. S. Giampapa (Tucson: Univ. Arizona Press), 1
 Wimmer Schweingruber, R. F., von Steiger, R., & Paerli, R. 1997, *J. Geophys. Res.*, in press